Journal of Materials Chemistry A

Accepted Manuscript

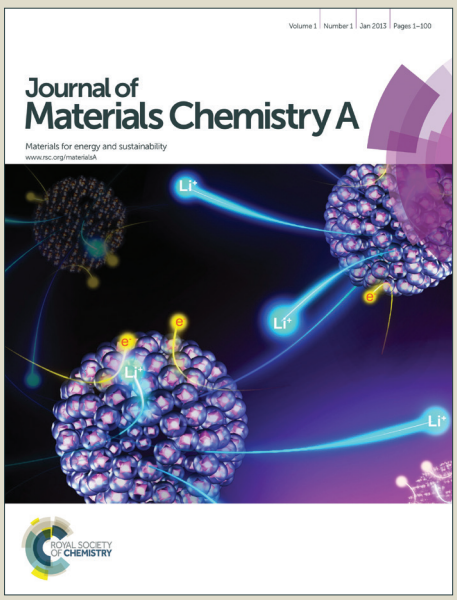

ROYAL SOCIETY OF CHEMISTRY

www.rsc.org/materialsA

Journal Name

COMMUNICATION

Highly Rate and Cycling Stable Electrode Materials constructed from Polyaniline/Cellulose Nanoporous Microspheres

Received 00th January 20xx,Accepted 00th January 20xx

DOI: 10.1039/x0xx00000x

www.rsc.org/

Dingfeng Xu,[a] Xu Xiao,[b] Jie Cai,[a] Jun Zhou [b]* and Lina Zhang [a]*

To resolve the problem of the pulverization and rapid capacity fading of the polymer electrode, novel electrode materials were constructed from polyaniline/cellulose microspheres (PANI/CM), which were fabricated *via in-situ* synthesis of PANI on cellulose matrix by using phytic acid (PA) as "bridge", for the first time. The constructing of the PANI/PA/CM successfully resolved the problem of the pulverization of PANI to be used as electrode materials. In our findings, the PANI subparticles with nanomesh structure were dispersed homogeneously in the cellulose microspheres from inside to outside, as a result of the firmly connecting between hydrophobic PANI and hydrophilic cellulose through the PA "bridge" to create micro- and nano-porous architecture. Meanwhile, the rest parts of PANI deposited on the surface of the microspheres to form a loose coralline structure, leading to the ion channels for the electrolyte penetration. The PANI/PA/CM composite electrodes exhibited excellent cycling stability (over 12000 cycles) and high rate capability, showing great potential in the energy-storage devices.

Faced with the impending energy crisis, the research on the high efficiency, low cost, environmentally friendly, and renewable energy resources has attracted much attentions.[1] Electrochemical capacitors, also known as supercapacitors (SCs), have significant potential as energy storage devices due to their unique properties, which includes but not limit to high power density, long cycle life, fast charge/discharge rates, and also low manufacturing costs.[2] Conductive polymers such as polyaniline (PANI), polypyrrole (PPy), and their derivatives are commonly used as pseudocapacitive electrode materials, owing to their facile synthesis and flexibility in processing and displaying high capacitance value.[3] However, the cycling performance of the PANI is poor due to the large volumetric swelling and shrinking during charge/discharge process as a result of ion doping and dedoping.[4] Thus, a number of efforts have been centred on improving their cycling stability such as adding of the graphene composite,[5] carbon nanotubes (CNT)[6] and hybrid with or electrochemically deposited onto transition metal oxides to achieve high-performance hybrid electrode materials.[7] The pulverization of PANI and rapid capacity fading of the polymer electrodes and their imperfect preparation including hazardous, time-consuming, or high cost limit their widespread application. Therefore, a deep development of high rate and cycling stable electrode materials *via* relatively simple, cost-effective, and green approaches is essential for their successful application.

It is worth noted that the theme of the spring 2015 ACS National Meeting was "Chemistry of Natural Resources". Cellulose is the most abundant renewable resource on the earth, and also one of the most intransigent macromolecule with moderate thermal stability.[8] Cellulose and its derivatives have been applied to many aspects, such as catalyst supports, electronics and biomaterials, where cellulose structure and properties have been thought very important.[9] Moreover, bacterial cellulose has been also used as support to fabricate conductive polymer/cellulose composites,[10] and the PANI/cellulose functional materials such as films, hydrogels and fibers have been fabricated from the PANI/cellulose solution in NaOH/urea aqueous solution in our laboratory.[11] Furthermore, the cellulose/Fe_3O_4 microspheres, and cellulose/TiO_2 microspheres have been constructed by using cellulose microspheres, which were prepared from the cellulose solution in NaOH/urea system, as a template via in-situ synthesis or by blending.[12] Additionally, the cellulose/PPy aerogels[13] and PANI/cellulose films[14] have been fabricated by using cellulose hydrogels as a template *via in-situ* synthesis. However, these materials could not simultaneously fulfill the requirements of electrochemical properties and cycling performance for energy-storage applications. Y. Cui et al have been reported that natural phytic acid (PA) has the phosphorus oxygen groups,[15] which can form a strong hydrogen-bonding with polyaniline to obtain excellent electrochemical activity materials. It is not hard to imagine that PA can form hydrogen-bond also with cellulose chains，thus it can create a "bridge" to simultaneously cross-link both PANI and cellulose, similar to "calcium bridge" in ionically crosslinked alginate.[16] Additionally, the *in-situ* polymerization can further result in the crosslinking the phytic acid "bridge" with aniline monomers to create a mesh-like PANI in the cellulose microspheres. Thus, constructing of the PANI/cellulose microspheres can resolve the problem of the pulverization.

Herein, for the first time, we demonstrated a large-scale and efficient strategy to construct the hydrogen-bonding-stabilized of polyaniline/cellulose nanoporous structure microspheres *via* phytic acid as "bridge", which was used as pseudocapacitance electrode

[a] D. Xu†, Prof.J.Cai, Prof. L. Zhang
College of Chemistry & Molecule Sciences, Wuhan University, Wuhan, 430072, China
E-mail: zhangln@whu.edu.cn
[b] X. Xiao†, Prof. J. Zhou
Wuhan National Laboratory for Optotelectronics, School of Optical and Electronic Information, Huazhong University of Science and Technology, Wuhan, 430074, China,
E-mail: jun.zhou@mail.hust.edu.cn
†These authors contributed equally to this work
†Electronic Supplementary Information (ESI) available: [details of any supplementary information available should be included here]. See DOI: 10.1039/x0xx00000x

materials. The cellulose was dissolved in 4.6 wt% LiOH/15 wt% urea aqueous system with cooling, which dissolves cellulose more easily than NaOH/urea aqueous solution.[17] The resulted cellulose solution was dropped in the Span 85 in isooctane with stirring *via* emulsifier to fabricate regenerated cellulose microspheres (CM). Subsequently, *in-situ* polymerization of aniline monomer occurred in the cellulose matrix at the presence of phytic acid to obtain largescale products of the polyaniline/cellulose nanoporous microspheres (Figure S1). Figure 1a-d shows the SEM images of the CM and their size distribution. The CM microspheres with relative narrow size distribution from 1 to 9 μm exhibited homogeneous porous structure with pore size ranged from about 100 to 200 nm, which was very useful as a micro-reactor for the polymerization of PANI. Figure 1 (e and h) shows SEM images of the. PANI/PA/CM and their size distribution. Obviously, the PANI with coralline pattern appeared on the surface of the CM, where the unlimited space induced the rapidly growing of the PANI aggregates to form loose structure with micro- and nano- pores, as a result of the unique role of attraction and repulsion of the hydrophilic phytic acid hydrogen bonded on the hydrophilic PANI chains. Thus, the size of the PANI/PA/CM was larger than that of CM, and the PANI/PA/CM exhibited a rough surface.

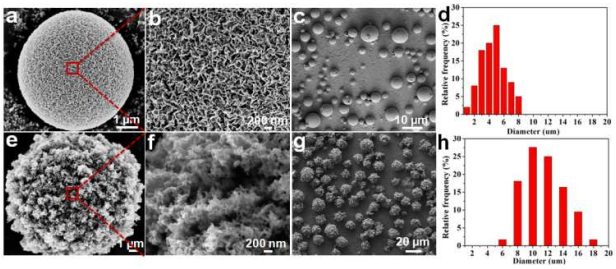

Figure 1. SEM image of a cellulose microsphere (CM) (a); high magnification SEM image of the surface (b); SEM image (c) and histogram of the size distribution (d) of the CM; SEM image of the PANI/PA/CM (e); a high magnification SEM image of the surface (f); SEM images (g) and histogram of the size distribution (h) of the PANI/PA/CM.

To characterize the inner, the PANI/PA/CM was cut into slices to be observed with the TEM images. Interestingly, the PANI loose nanoparticles (mean size of proximately 100 nm) constituted of nanofibers their exhibited uniform 3D mesh structure, and were dispersed homogeneously in the CM from inside to outside, as shown in Figure 2a and 2b. The nano-porous structure of the cellulose matrix supplied not only cavities for the *in-situ* synthesis of PANI, but also a shell to protect the growing of the PANI aggregates in the microsphere. It is worth noting that in our previous work, the proportion of PANI in PANI/CNT/cellulose composite films decreases with the depth increase, as a result of the slow diffusion of the aniline in the interior.[12] However, in this work, the PANI nanoparticles were homogeneously dispersed in the CM from surface to inner, owing to the doping phytic acid, which induced the uniform diffusion of the aniline in the CM, droved by the hydrogen bonds. In our findings, the phytic acid could not only connect firmly with both PANI and cellulose to create micro- and nano-porous architecture, but also as a doping agent of PANI. Figure 2 (c~d) shows the nitrogen adsorption and desorption isotherms as well as Barrett–Joyner–Halendar (BJH) pore size distribution of the CM and PANI/PA/CM. These microspheres exhibited a type I H3 hysteresis loop according to the IUPAC and BDDT classification, as the adsorption branch was parallel to P/P_0 over a large extent. The Brunauer-Emmett-Teller (BET) surface area of the CM and PANI/PA/CM were calculated to be ~ 176 m^2/g and ~ 152 m^2/g, respectively. The pore size distribution indicated that the PANI/PA/CM had smaller mesopores, approximately 8 nm at peak

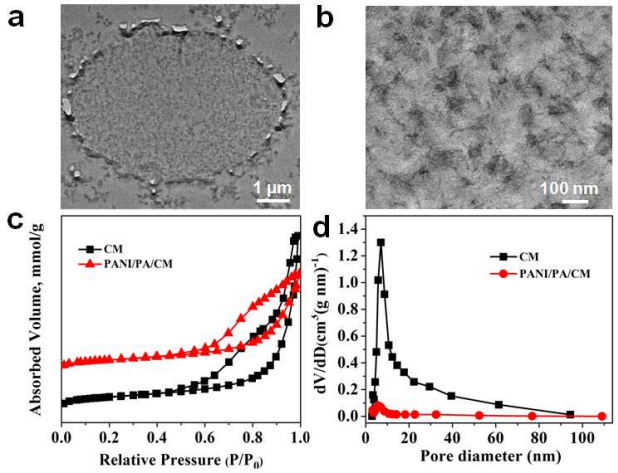

Figure 2. TEM image of a PANI/PA/CM (a); a high magnification TEM image of inside(b); nitrogen adsorption and desorption isotherms (c) and Barrett–Joyner–Halendar (BJH) pore size distribution of cellulose microspheres (CM) and PANI/PA/CM (d).

maximum (Figure 2d). These results further confirmed the occupying of PANI in the pore of the CM, resulting in a decrease of the pore size and BET.

To further confirm the existence of strong hydrogen bonding between phytic acid with the –OH of cellulose and the –NH of PANI, the CM and PANI/PA/CM were investigated with the solid-state cross-polarization/magic-angle spinning (CP/MAS) ^{13}C NMR (Figure 3a) and ^{13}P NMR (Figure S4b) spectra. The CM displayed characteristic chemical shifts at 106.1, 88.4, 75.3, and 63.3 ppm, respectively, assigning to the C1, C3, C2 and C6 of cellulose Ⅱ.[18] As a result of the possible hydrogen-bond interactions between the phytic acid with the –OH of cellulose and the –NH of PANI, the chemical shifts of C2, C3 and C6 for cellulose in the PANI/PA/CM shifted to upfield by about 1 ppm as well as the intensity of the shoulder peak for the C4 carbon (amorphous regime) significantly enhanced, compared with the CM, suggesting the weakening of the hydrogen bonding of cellulose themselves by the formation of new hydrogen bonds between the three components. Furthermore, ^{13}P NMR spectrum of the PANI/PA/CM (Figure S4b) was compared with that of the pure phytic acid (Figure S4a).[19] There are five symmetrical signals in ^{31}P fast-MAS NMR spectrum of the phytic acid due to the ^{31}P-D spin-spin coupling. However, the multiple signals of ^{31}P of the PANI/PA/CM became less, which could be attributed to the changed chemical environments of P atoms, indicating the presence of strong interaction between phytic acid with cellulose and PANI. Figure 3b shows the Fourier transform infrared spectroscopy (FTIR) of the PANI, CM and PANI/PA/CM. The peak at 3300-3500 cm^{-1} was corresponded to the stretching absorption peak of O-H of cellulose, and its intensity was much weaker in the PANI/PA/CM than that in the CM, indicating that the native hydrogen bonding in cellulose was broken by the incorporation of phytic acid and PANI. The broad bands around 1304 and 1237 cm^{-1} were attributed to C-N and C=N stretching vibration characteristic absorption peak of PANI, respectively,[20] indicating the existence of PANI in the PANI/PA/CM. The conclusion was also supported by the results from X-ray photoelectron spectroscopy (XPS) (Figure S5), wide-angle X-ray diffraction (WAXD) and thermal gravimetric analysis (FigureS6).[21] Furtherer, the TG curves (Figure S6) indicated that the thermal stability of the PANI/PA/CM was higher than that of the CM, which

was related with the strong hydrogen bonding interaction between phytic acid, cellulose and PANI.

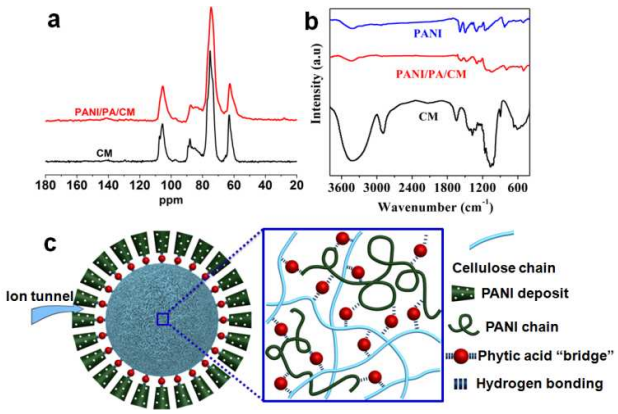

Figure 3. Solid-state CP/MAS ^{13}C NMR spectra (a) and FT-IR spectra (b) of the PANI, PANI/PA/CM and cellulose microspheres (CM); a schematic of the PANI/PA/CM (left, c) and architecture of the hydrogen bonded PANI/PA/cellulose complex through phytic acid "bridge" (right, c).

On the basis of the above experimental results and theoretic analysis, a possible mechanism for the construction of the PANI/PA/CM is proposed in Figure 3 (c, left). There were many nanopores with 100 ~ 200 nm in the CM, supported by the results in Figure 1 (a and b). The PANI chains were immobilized in the backbones of the CM *via* phytic acid "bridge", as shown in Figure 3 (c, right), supported by the results in Figures 2 (a and b), 3 (a and b), and S4-S6. In our findings, the phytic acid served as a "bridge" played an important role in the firmly fixing of the PANI chains in the regenerated CM matrix through hydrogen bonds as well as the formation of the homogeneous porous architecture of the PANI/PA/CM. As shown in Figure 3 (c, left), the PANI deposits on the surface of the CM formed coralline porous architecture, supported by the results in Figures 2a and S3c. The PANI component with micro- and nano-porous structure could provide ion channels for the penetration of electrolyte, whereas cellulose contributed affinity on sulfuric acid electrolyte, this was very important in the electrode materials.

To evaluate the electrochemical performances of the PANI/PA/CM, test was first performed in 1 M H_2SO_4 in three-electrode configurations with activated carbon as the counter electrode and Ag/AgCl as the reference electrode. The electrodes were composed of 80 wt% PANI/PA/CM, 10 wt% acetylene black (Alfa Aesar, 99.9%), and 10 wt% polytetrafluoroethylene (PTFE) as a binder to be flexible circular electrodes (Figure S2). In the cyclic voltammetry (CV) curves (Figure 4a), two pairs of redox peaks were apparently displayed which correspond to the leucoemeraldine/emeraldine and emeraldine/pernigraniline transitions of PANI, revealing the pseudocapacitance behavior of PANI. Moreover, the electrodes exhibited very fast current responses within 4 s at the switching potentials (-0.1 V and 0.7 V), which could be attributed to the high conductivity. It was worth noting that the sheet resistance of the PANI/PA/CM was measured to be 6.0-6.5 Ω/sq. The good conductivity could also be observed from the electrochemical impedance spectroscopy (EIS), as shown in Figure 4b. A small semi-circle of about 3.5 Ω appeared in low-frequency region, indicating a low charge transfer resistance. Moreover, the EIS of pure PANI was about 12.5 Ω (Figure S7), which was larger than that of PANI/PA/CM. Considering that charge transfer resistance is a combination of electron and ion conductivity, both of

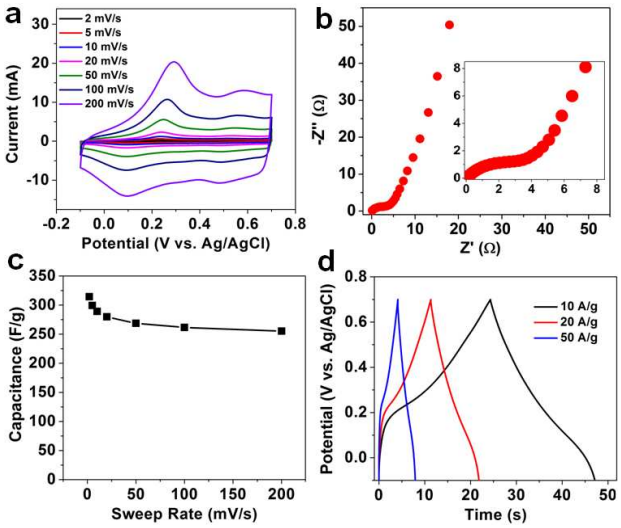

Figure 4. Electrochemical performances in three-electrode configurations: CV curves of PANI/PA/CM electrode under sweep rate from 2 to 200 mV/s (a); EIS spectrum (b); capacitance versus sweep rate (c); GCD curves under high current density of 10, 20 and 50 A/g (d).The inset shows the charge transfer resistance.

the PANI/PA/CM structure and the nanopores contributed to this good performance of the PANI/PA/CM. Firstly, the superior affinity between cellulose and electrolyte could assure the PANI/PA/CM to serve as a reservoir, adsorbing large amount of ions around the electrodes. Secondly, micro- and nano-porous architecture of the PANI/PA/CM could facilitate the permeation of the ions, accelerating the ion diffusion. Finally, the coralline PANI deposits on the surface and the inner mesh structure of the PANI/PA/CM provided a stable tunnel for fast proton transport. It is expected that this material could provide excellent power handling properties which is the most important feature of supercapacitors. To demonstrate our hypothesis, the curve of capacitance versus sweep rate is shown in Figure 4c, which was obtained *via* equation: $\int(IV)/(mv\Delta V)$ from the CV curves in Figure 4b. At a low sweep rate of 2 mV/s, the specific capacitance was 314 F/g, and at a low current density of 1.1A/g, the specific capacitance was 349 F/g in the curve of capacitance versus current density (Figure S8). These results indicated the good specific capacitance of PANI/PA/CM. Surprisingly, at a high sweep rate of 200 mV/s (charge/discharge time for 4 s), the capacitance was still 255 F/g which was 81.2% retention of capacitance from 2 to 200 mV/s. Such a high rate capability was superior to that of the most recently reported PANI/carbon composite electrode, such as PANI/graphene composite paper (64.2 % of capacitance retention with the current density increase from 1 A/g to 10 A/g) and PANI coated on graphitized carbon nanofibers (52 % capacitance retention with the current density increase from 0.4 A/g to 50 A/g). Given that cellulose gives no contribution to the capacitance due to the insulation, and the mass loading of PANI was not low (~ 1 mg/cm^2), such an excellent rate capability could be only attributed to the featured porous structure, affinity between cellulose and electrolyte, and hydrogen bonded "bridge". The high rate properties could also be testified by galvanostatic charge-discharge (GCD) tests. As shown in Figure 4d, the GCD curves were almost symmetric and even displayed a small *IR* drop at a high current density of 50 A/g.

For application consideration, two-electrode setup measurement is of more significance. Here, a device was fabricated by sandwiching two identical electrodes with a separator, and the electrolyte was still

1 M H_2SO_4. From the normalized CV curves as shown in Figure 5a, the area of CV curves changed hardly, suggesting a good rate capability. GCD curves from 0.5 to 20 A/g are shown in Figure 5b. From the symmetric profiles with small IR drop in the GCD curves the PANI/PA/CM electrodes exhibited good conductivity. Figure 5c shows the gravimetric capacitance under the sweep rate from 2 to 100 mV/s. At a low sweep rate of 2 mV/s, the gravimetric capacitance was only 65 F/g. Similarly with the three-electrode measurement, the device revealed an excellent rate capability with 70% capacitance retention. In addition, the highest energy density is 5.8 Wh/kg with a power density of 130 W/kg. Importantly, the device could deliver a high power density of 1783 W/kg with an energy density of 4 Wh/kg (Figure S9).

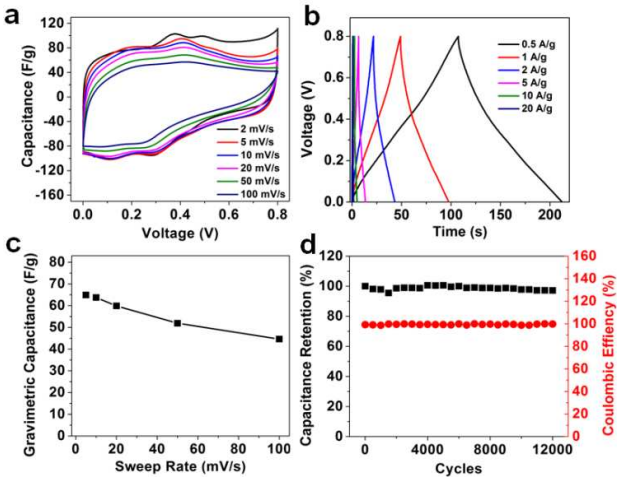

Figure 5. Electrochemical performance for a two-electrode device with PANI/PA/CM films as the electrodes: normalized CV curves under sweep rate from 2 to 100 mV/s (a); GCD curves under current density from 0.5 to 20 A/g (b); capacitance versus sweep rate (c); cycling stability and coulombic efficiency for 12000 cycles under 2 mA (d).

Since the first invention of PANI,[22] the constraint of its industrial application is the poor cycling stability. The swelling and contraction of PANI during charging/discharging, which results in the fracture of PANI chains, is the main reason for the cycling degradation. Here, in our findings, a very strong and tough connection between PANI and cellulose provided by the phytic acid "bridge", and the micro- and nano-porous structure led to the electrochemical stability of PANI. As shown in Figure 5d, no apparent degradation of PANI could be observed after 12000 cycles with high coulombic efficiency of around 100 %. This excellent cycling stability of PANI/PA/CM was much better than the common values of PANI or PANI/carbon composite electrodes, (Table S1) and the cycling stable capability was higher by 12 times than that of PANI/CNT/cellulose films in our previous work.[14] Yushin *et al.* [23] have reported an excellent PANI/multifunctional CNT composite electrodes with stability of 30000 cycles, which needed an additive multifunctional CNT as the scaffold. In our findings, the PANI/PA/CM based device without any inorganic additives had the excellent cycling stability, high rate capability and good conductivity. This could be owing to the unique role of the hydrogen bonded phytic acid "bridge". By virtue of the low cost and easy synthesis procedure, it is reasonable to expect that the PANI/PA/CM electrodes have both of scientific and industrial merits.

In summary, PANI was *in-situ* synthesized in the regenerated cellulose microspheres, which were prepared from the cellulose in LiOH/urea aqueous solution, to construct novel PANI/PA/CM electrode materials with phytic acid as "bridge". The PANI/PA/CM successfully resolved the problem of the pulverization of PANI to be used as electrode materials. The phosphorus oxygen groups in the phytic acid could form strong hydrogen bonding with both the cellulose and PANI, leading to firmly fix the PANI chains on the cellulose template. The PANI subparticles with nanomesh structure were dispersed homogeneously in the cellulose microspheres from inside to outside, as a result of the firmly connecting between hydrophobic PANI and hydrophilic cellulose through hydrogen bonds to create micro- and nano-porous architecture. The rest part of PANI deposited on the surface of the microspheres to form a loose coralline structure, leading to the good ion channel for the penetration of electrolyte. The PANI/PA/CM exhibited excellent cycling stability (over 12000 cycles), high rate capability and good conductivity as electrode materials. The superior affinity of cellulose with electrolyte, the homogeneous micro- and nano-porous architecture, large specific surface area of the PANI/PA/CM played an important role in achieving such a high electrochemical performance. This work provided a novel, large-scale and cost-efficient strategy to construct the highly efficient electrode materials, which would have potential applications in energy storage.

Acknowledgements
This work was financially supported by the National Basic Research Program of China (973 Program, 2010CB732203), the Major Program of National Natural Science Foundation of China (21334005), the Natural Science Foundation of China (51322210, 61434001, 21422405). The authors thank to the support of the Center for Nanoscale Characterization & Devices (CNCD), WNLO-HUST and the Analysis and Testing Center of Huazhong University of Science and Technology.

Notes and references

1 (a) J. E. Trancik, Nature, 2014, **507**, 300; (b) H. Williams, A. De Benedictis, R. Ghanadan, A. Mahone, J. Moore, W. R. Morrow III, S. Price and M. S. Torn, Science, 2012, **335**, 53; (c) N. Armaroli and V. Balzani, Angew. Chem. Int. Ed., 2007, **46**, 52; (d) M. Carbajales-Dale, C. J. Barnhart and S. M. Benson, Energy Environ. Sci., 2014, **7**, 1538.
2 (a) P. Simon and Y. Gogotsi, Nat. Mater., 2008, **7**, 845; (b) X. L. Wu, L. Y. Jiang, F. F. Cao, Y. G. Guo and L. J. Wan, Adv. Mater., 2009, **21**, 2710; (c) Y. Yang, H. Fei, G. Ruan, C. Xiang and J. M. Tour, Adv Mater., 2014, **26**, 8163.
3 (a) D. Ge, L. Yang, L. Fan, C. Zhang, X. Xiao, Y. Gogotsi and S. Yang, Nano Energy, 2015, **11**, 568; (b)Y. Yang, Y. Hao, J. Yuan, L. Niu and F. Xia, Carbon, 2014, **78**, 279; (c) W. Zhou, Y. Yu, H. Chen, F. J. Disalvo and H. D. Abruna, J. Am. Chem. Soc., 2013, **135**, 16736; (d) S. Li, D. Huang, J. Yang, B. Zhang, X. Zhang, G. Yang, M. Wang and Y. Shen, Nano Energy, 2014, **9**, 309.
4 (a) S. Giri, D. Ghosh and C. K. Das, Adv. Funct. Mater., 2014, **24**, 1312; (b) D. Vonlanthen, P. Lazarev, K. A. See, F. Wudl and A. J. Heeger, Adv Mater., 2014, **26**, 5095.
5 M. Yu, Y. Ma, J. Liu and S. Li, Carbon, 2015, **87**, 98.
6 T. Liu, L. Finn, M. Yu, H. Wang, T. Zhai, X. Lu, Y. Tong and Y. Li, Nano Lett., 2014, **14**, 2522.
7 (a) S. Li, D. Wu, C. Cheng, J. Wang, F. Zhang, Y. Su and X. Feng, Angew. Chem. Int. Ed., 2013, **52**, 12105; (b) C. Lu, T. Ben, S. Xu and S. Qiu, Angew. Chem. Int. Ed., 2014, **53**, 6454; (c) J. Zang and X. Li, J. Mater. Chem., 2011, **21**, 10965; (d) X. Zhang, X. Zeng, M. Yang and Y. Qi, ACS Appl. Mater. Interfaces., 2014, **6**, 1125.
8 (a) H. Wang, G. Gurau and R. D. Rogers, Chem Soc Rev., 2012, **41**, 1519; (b) S. Zhu, Y. Wu, Q. Chen, Z. Yu, C. Wang, S. Jin, Y. Ding and G. Wu, Green Chem., 2006, **8**, 325.
9 (a) C. M. Cirtiu, A. F. Dunlop-Brière and A. Moores, Green Chem., 2011, **13**, 288; (b) Z. Gui, H. Zhu, E. Gillette, X. Han, G. W. Rubloff, L. Hu and S. Lee, ACS Nano, 2013, **7**, 6037; (c) S. Dong and M. Roman, J. Am. Chem. Soc., 2007, **129**, 13810; (d) M. M. Malinen, L. K. Kanninen, A. Corlu, H. M. Isoniemi, Y. R. Lou, M. L. Yliperttula and A. O. Urtti, Biomaterials, 2014, **35**, 5110; (e) R. J. Moon, A. Martini, J. Nairn, J. Simonsen and J. Youngblood, Chem Soc Rev., 2011, **40**, 394; (f) L. Zhang, Z. Liu, G. Cui and L. Chen, Prog Polym Sci., 2015, **43**, 136.

10 (a) S. Li, D. Huang, B. Zhang, X. Xu, M. Wang, G. Yang and Y. Shen, Adv. Energy Mater., 2014, **4**, 1; (b) C. Long, D. Qi, T. Wei, J. Yan, L. Jiang and Z. Fan, Adv. Funct. Mater., 2014, **24**, 3953; (c) H. Wang, L. Bian, P. Zhou, J. Tang and W. Tang, J. Mater. Chem. A, 2013, **1**, 578.
11 (a) X. Shi, L. Zhang, J. Cai, G. Cheng, H. Zhang, J. Li and X. Wang, Macromolecules, 2011, **44**, 4565; (b) X. Shi, Y. Hu, K. Tu, L. Zhang, H. Wang, J. Xu, H. Zhang, J. Li, X. Wang and M. Xu, Soft Matter, 2013, **9**, 10129; (c) X. Shi, Y. Hu, F. Fu, J. Zhou, Y. Wang, L. Chen, H. Zhang, J. Li, X. Wang and L. Zhang, J. Mater. Chem. A, 2014, **2**, 7669.
12 (a) X. Luo, S. Liu, J. Zhou and L. Zhang, J. Mater. Chem., 2009, **19**, 3538; (b) J. Duan, X. He and L. Zhang, Chem. Commun., 2015, **51**, 338.
13 Z. Shi, H. Gao, J. Feng, B. Ding, X. Cao, S. Kuga, Y. Wang, L. Zhang and J. Cai, Angew. Chem. Int. Ed., 2014, **53**, 5380.
14 X. Shi, Y. Hu, M. Li, Y. Y. Duan, Y. Wang, L. Chen and L. Zhang, Cellulose, 2014, **21**, 2337.
15 (a) L. Pan, G. Yu, D. Zhai, H. R. Lee, W. Zhao, N. Liu, H. Wang, B. C.-K. Tee, Y. Shi, Y. Cui and Z. Bao, PNAS, 2012, **109**, 1; (b) B. Liu, P. Soares, C. Checkles, Y. Zhao and G. Yu, Nano Lett., 2013, **13**, 3414; (c) L. Pan, A. Chortos, G. Yu, Y. Wang, S. Isaacson, R. Allen, Y. Shi, R. Dauskardt and Z. Bao, Nat. Commun., 2014, **5**, 1; (d) H. Wu, G. Yu, L. Pan, N. Liu, M. T. McDowell, Z. Bao and Y. Cui, Nat. Commun., 2013, **4**, 1; (e) J. F.Mike and J. L. Lutkenhaus, ACS Macro Lett., 2013, **2**, 839; (f) Y. Zhao, B. Liu, L. Pan and G. Yu, Energy Environ. Sci., 2013, **6**, 2856.
16 J. Sun, X. Zhao, W. Illeperuma, O. Chaudhuri, D. Mooney, J. Vlassak and Z. Suo, Nature, 2012, **489**, 133.
17 J. Cai and L. Zhang, Macromol. Biosci., 2005, **5**, 539.
18 Q. Wang, J. Cai, L. Zhang, M. Xu, H. Cheng, C. C. Han, S. Kuga, J. Xiao and R. Xiao, J. Mater. Chem. A, 2013, **1**, 6678.
19 G. Mali, M. Sala, I. Arcon, V. Kaucic and J. Kolar, J. Phys. Chem. B, 2006, **110**, 23060.
20 X. Li, Y. Liu, W. Guo, J. Chen, W. He and F. Peng, Electrochim. Acta, 2014, **135**, 550.
21 (a) Y. Zhu, D. Hu, M. X. Wan, L. Jiang and Y. Wei, Adv. Mater., 2007, **19**, 2092; (b) M. Kim, C. Lee and J. Jang, Adv. Funct. Mater., 2014, **24**, 2489; (c) C. H. B. Silva, A. M. Da Costa Ferreira, V. R. L. Constantino and M. L. A. Temperini, J. Mater. Chem. A, 2014, **2**, 8205.
22 A.G. Macdiarmid, J.C. Chiang and A.F. Richter, Synthetic Met., 1987, **18**, 285.
23 J. Benson, I. Kovalenko, S. Boukhalfa, D. Lashmore, M. Sanghadasa and G. Yushin, Adv. Mater., 2013, **25**, 6625.

Highly Rate and Cycling Stable Electrode Materials constructed from Polyaniline/Cellulose Nanoporous Microspheres

Dingfeng Xu,[a] Xu Xiao,[b] Jie Cai,[a] Jun Zhou [b]* and Lina Zhang [a]*

Graphical abstract

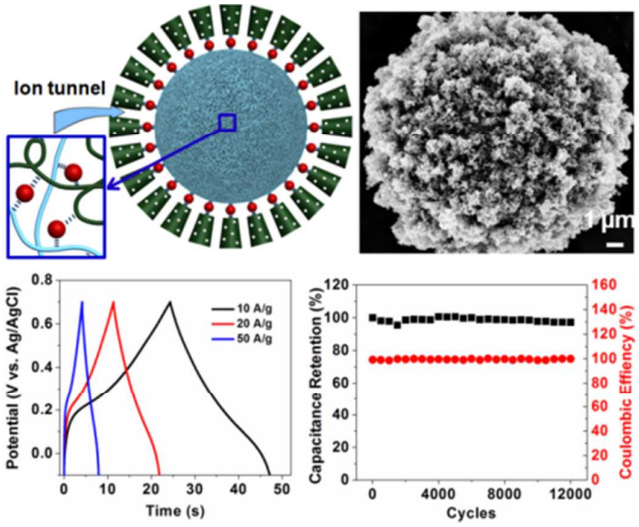

Highly efficient electrode materials were constructed from polyaniline/cellulose microspheres (PANI/PA/CM) *via* phytic acid (PA) as "bridge" through hydrogen bonding. The electrodes exhibited excellent cycling stability and high rate capability, as a result of the superior affinity of cellulose with electrolyte and the homogeneous nanoporous architecture, leading to good ion channels.